

# Discriminating Different $Z'$ s via Asymmetries at the LHC

Zhong-qiu Zhou<sup>1a</sup>, Bo Xiao<sup>1b</sup>, You-kai Wang<sup>1c</sup>, Shou-hua Zhu<sup>1,2d</sup>

<sup>1</sup> *Institute of Theoretical Physics & State Key Laboratory of Nuclear Physics and Technology,*

*Peking University, Beijing 100871, China*

<sup>2</sup> *Center for High Energy Physics, Peking University, Beijing 100871, China*

(Dated: January 11, 2013)

---

<sup>a</sup> E-mail:zhongqiu\_zhou@pku.edu.cn

<sup>b</sup> E-mail:homenature@pku.edu.cn

<sup>c</sup> E-mail:wangyk@pku.edu.cn

<sup>d</sup> E-mail:shzhu@pku.edu.cn

## Abstract

In practice the asymmetry, which is defined based on the angular distribution of the final states in scattering or decay processes, can be utilized to scrutinize underlying dynamics in and/or beyond the standard model (BSM). As one of the possible BSM physics which might be discovered early at the LHC, extra neutral gauge bosons  $Z'$ 's are theoretical well motivated. Once  $Z'$ 's are discovered at the LHC, it is crucial to discriminate different  $Z'$ 's in various BSM. In principle such task can be accomplished by measuring the angular distribution of the final states which are produced via  $Z'$ -mediated processes. In the real data analysis, asymmetry is always adopted. In literature several asymmetries have been proposed at the LHC. Based on these works, we stepped further on to study how to optimize the asymmetries in the left-right model and the sequential standard model, as the examples of BSM. In this paper, we examined four kinds of asymmetries, namely rapidity-dependent forward-backward asymmetry, one-side forward-backward asymmetry, central charge asymmetry and edge charge asymmetry (see text for details), with  $\ell^+\ell^-$  ( $\ell = e, \mu$ ),  $b\bar{b}$  and  $t\bar{t}$  as the final states. In the calculations with  $b\bar{b}$  and  $t\bar{t}$  final states, the QCD-induced higher order contributions to the asymmetric cross section were also included. For each kind of final states, we estimated the four kinds of asymmetries and especially the optimal cut usually associated with the definition of the asymmetry. Our numerical results indicated that the capacity to discriminate  $Z'$  models can be improved by imposing the optimal cuts.

## I. INTRODUCTION

LHC is a powerful machine for discovering new particle and examining its couplings if the new particle is at  $\mathcal{O}(\text{TeV})$  or below. In the physics beyond the standard model (BSM), there are usually new particles. For example in the simplest case, besides the standard model (SM) gauge group  $SU(3)_C \otimes SU(2)_L \otimes U(1)_Y$ , there can be an extra abelian gauge group  $U(1)$  which implies the existence of the extra gauge boson dubbed as  $Z'$ . If the mass of  $Z'$  is not so heavy, it can be discovered early at the LHC. Similar to the case of  $J/\psi$  discovery,  $Z'$  might show up as the di-muon resonance. In fact numerous phenomenological studies on  $Z'$  at the LHC have been carried out. After the discovery it is very important to study its spin, couplings etc. in order to fix the nature of the physics behind the new particle. In principle such detail information can be obtained via the precise measurement for the angular distributions of the final states into which  $Z'$ 's decay. However in practice the asymmetry is usually utilized to investigate the detail properties of the new particle, provided that the data sample is usually limited in the real experiments. The measurement of the asymmetry at the LEP (Tevatron), as the charge asymmetric electron-positron (proton-antiproton) collider, has shed light on the knowledge of the SM and constrained the BSM severely. The LHC, as the charge symmetric proton-proton collider, has unique feature to define and measure the asymmetry.

In literature, several asymmetry definitions have already been proposed to study the underlying dynamics of the BSM. Note that asymmetry is applicable to all kinds of new physics, not limited to  $Z'$ . In this paper  $Z'$  is only taken as an example. In order to distinguish different  $Z'$  models, forward-backward asymmetry at the hadron collider is one of the most important tools which was suggested in 1984 in the study of  $Z'$  physics [1]. Afterwards, it was widely used in the  $Z'$  study [2–28] and has been developed into more convenient forms. In fact at the LHC, there are several other types of asymmetry definitions [29–35]. It is crucial to compare them and find out the most suitable one for the specific purpose, eg. to study the specific couplings between  $Z'$  and the SM fermions. Furthermore, each type of asymmetry definition contains characteristic cuts which should be chosen properly to make the asymmetry most significant. The most suitable type of asymmetry and the most proper cuts associated with asymmetry are different for different physics. In this paper, we are going to investigate the optimal cuts for identifying the  $Z'$  in different models at the LHC.

In this paper two kinds of  $Z'$  test models namely the left-right (LR) and sequential standard model (SSM) are adopted.

In the previous study [8], the authors utilized the forward-backward asymmetry defined by themselves in order to identify the different  $Z'$ s, which can decay into  $\mu^+\mu^-(e^+e^-)$ ,  $b\bar{b}$  as well as  $t\bar{t}$ . For the final states of  $\mu^+\mu^-(e^+e^-)$ , asymmetry is calculated for the on-peak data sample namely the invariant mass of the charged lepton pair lying within  $M_{Z'} - 3\Gamma$  and  $M_{Z'} + 3\Gamma$ , as well as the off-peak data sample with invariant mass lying within  $2/3M_{Z'}$  and  $M_{Z'} - 3\Gamma$ . Here  $\Gamma$  is the total width of  $Z'$ . For the  $b\bar{b}$  and  $t\bar{t}$  final states, only asymmetry of on-peak data sample with quark pair invariant mass within  $M_{Z'} - 2.5\Gamma$  and  $M_{Z'} + 2.5\Gamma$  was calculated. In this paper we extended the above analysis to more asymmetries defined recently, namely one-side forward-backward asymmetry, central charge asymmetry and edge charge asymmetry. In our calculation for the quarks as the final states, we included also the contributions from the higher-order QCD-induced effects. Moreover we investigated the optimal conditions which make the asymmetry more significant. Explicitly, in our paper we are going to scrutinize which type of asymmetry and the corresponding cuts are the most suitable ones for the  $\mu^+\mu^-(e^+e^-)$  on/off-peak events the  $b\bar{b}$  and  $t\bar{t}$  events respectively.

In section II, different asymmetries at the LHC are briefly described. In section III, we firstly calculated four types of asymmetries at the LHC with their characteristic cuts for the  $\mu^+\mu^-(e^+e^-)$  on/off-peak events,  $b\bar{b}$ ,  $t\bar{t}$  on-peak events respectively. Secondly, based on the calculations we optimize the asymmetry for each case by choosing different cuts. Thirdly, we showed how to discriminate different  $Z'$ s in LR and SSM models utilizing the optimized asymmetry. In section IV, we gave our discussions and conclusions.

## II. ASYMMETRY AT THE LHC

LHC is the *symmetric* proton-proton collider, thus the usual defined asymmetry is absolute zero after integrating all kinematical region. However if one selects events in a certain kinematical region, the asymmetry arising at partonic level will be kept.

### A. Forward-backward asymmetry for the partonic level process $q\bar{q} \rightarrow f\bar{f}$

In order to illustrate the  $Z'$  contribution to asymmetry, we describe firstly the forward-backward (FB) asymmetry in the SM. At the tree level in the SM, the FB asymmetry of  $q\bar{q} \rightarrow Z/\gamma^* \rightarrow l\bar{l}$  gets contributions from the self conjugation of the Z-induced s-channel feynman diagram

$$\frac{d\sigma}{d\cos\theta} \propto \frac{g^4 s^2}{c_W^4 [(s - M_Z^2)^2 + \Gamma_Z^2 M_Z^2]} [((g_L^l)^2 + (g_R^l)^2)((g_L^q)^2 + (g_R^q)^2)(1 + \cos^2\theta) + 2((g_L^l)^2 - (g_R^l)^2)((g_L^q)^2 - (g_R^q)^2)\cos\theta], \quad (1)$$

and the interference between this diagram and the  $\gamma$ -induced s-channel feynman diagram

$$\frac{d\sigma}{d\cos\theta} \propto \frac{g^2 ee_q (M_Z^2 - s)s}{c_W^2 [(s - M_Z^2)^2 + \Gamma_Z^2 M_Z^2]} [2(g_L^l + g_R^l)(g_L^q + g_R^q)(1 + \cos^2\theta) + 4(g_L^l - g_R^l)(g_L^q - g_R^q)\cos\theta]. \quad (2)$$

Around the Z-pole, the FB asymmetry is almost determined by the first contribution, while off the Z-pole, the second contribution plays an important role.

After introducing  $Z'$ , the situation becomes a little bit complicated. On the  $Z'$  pole, if the coupling of the  $Z'$  to fermions is *not* pure vector-like nor pure axial-vector-like namely  $|g_L^f| = |g_R^f|$ , there will be non-zero contribution to FB asymmetry from the self-conjugation of the  $Z'$  induced s-channel feynman diagram. Otherwise contribution from self-conjugation of  $Z'$  to F-B asymmetry will be zero. However for the data sample off the  $Z'$  pole, FB asymmetry will be non-zero due to the interference of the  $Z'$  diagram and the SM  $Z/\gamma^*$  induced s-channel feynman diagrams.

From the above description, we can see clearly that the FB asymmetry relates tightly to the chiral properties of the couplings and how to select data samples. In the BSM which contains the  $Z'$ , the coupling of  $Z'$  and SM fermions is usually different. How to extract the corresponding couplings via asymmetry measurement and subsequently discriminate different BSM is the key motivation for both the theoretical and experimental studies.

The above formulas are applicable also to  $q\bar{q} \rightarrow b\bar{b}(t\bar{t})$ , however there are additional important contributions to the F-B asymmetry from the QCD high-order processes [29, 30]. If one selects the events around the  $Z'$  pole, the QCD high-order contributions are suppressed. However such effect will be important for the asymmetry of off-pole events. In this paper, such QCD-induced contributions will be included in the analysis.

### B. Four asymmetries defined at the LHC

The proton-proton collider LHC is forward-backward charge symmetric, so the asymmetry of the fermion pairs produced at the LHC is null if integrating over the full phase space. However, by imposing some kinematical cuts, the asymmetry generated at the partonic level  $q\bar{q} \rightarrow f\bar{f}$  can be kept. Different types of asymmetries have been defined. The above-mentioned FB asymmetry [1–10] which have been frequently used in  $Z'$  studies contains a characteristic fermion pair rapidity  $Y_{f\bar{f}}$  cut. We refer it as rapidity dependent forward-backward asymmetry ( $A_{\text{RFB}}$ ) throughout this paper. The other three asymmetries which will be investigated in this paper are one-side forward-backward asymmetry ( $A_{\text{OFB}}$ ) [33, 34], central charge asymmetry ( $A_{\text{C}}$ ) [29–32], and edge charge asymmetry ( $A_{\text{E}}$ ) [35]. We collect their definitions as below

$$A_{\text{RFB}}(Y_{f\bar{f}}^{\text{cut}}) = \frac{\sigma(|Y_f| > |Y_{\bar{f}}|) - \sigma(|Y_f| < |Y_{\bar{f}}|)}{\sigma(|Y_f| > |Y_{\bar{f}}|) + \sigma(|Y_f| < |Y_{\bar{f}}|)} \Big|_{|Y_{f\bar{f}}| > Y_{f\bar{f}}^{\text{cut}}}, \quad (3)$$

$$A_{\text{OFB}}(p_{Z,f\bar{f}}^{\text{cut}}) = \frac{\sigma(|Y_f| > |Y_{\bar{f}}|) - \sigma(|Y_f| < |Y_{\bar{f}}|)}{\sigma(|Y_f| > |Y_{\bar{f}}|) + \sigma(|Y_f| < |Y_{\bar{f}}|)} \Big|_{|p_{z,f\bar{f}}| > p_{Z,f\bar{f}}^{\text{cut}}}, \quad (4)$$

$$A_{\text{C}}(Y_{\text{C}}) = \frac{\sigma_f(|Y_f| < Y_{\text{C}}) - \sigma_{\bar{f}}(|Y_{\bar{f}}| < Y_{\text{C}})}{\sigma_f(|Y_f| < Y_{\text{C}}) + \sigma_{\bar{f}}(|Y_{\bar{f}}| < Y_{\text{C}})}, \quad (5)$$

$$A_{\text{E}}(Y_{\text{C}}) = \frac{\sigma_f(Y_{\text{C}} < |Y_f|) - \sigma_{\bar{f}}(Y_{\text{C}} < |Y_{\bar{f}}|)}{\sigma_f(Y_{\text{C}} < |Y_f|) + \sigma_{\bar{f}}(Y_{\text{C}} < |Y_{\bar{f}}|)} \quad (6)$$

in which  $Y$  is the rapidity of  $f/\bar{f}$  or fermion pair accordingly. The  $p_{z,f\bar{f}}$  is the z-direction momentum of the fermion pair.

In order to keep the partonic asymmetry even at the hadronic level, no matter how different these asymmetries look like, each of them has used the fact that the energy fraction of the valence quark is usually larger than that of the sea quark in the proton. These asymmetries can be classified into two categories according to their similarities.  $A_{\text{C}}$  and  $A_{\text{E}}$  belong to one category and the remaining two belong to the other. For  $A_{\text{C}}$  and  $A_{\text{E}}$ , they account two complementary kinematical regions, namely central region  $|Y_{f,\bar{f}}| < Y_{\text{C}}$  and the edge region  $|Y_{f,\bar{f}}| > Y_{\text{C}}$  in the laboratory frame respectively.  $A_{\text{E}}$  can usually suppress more efficiently the symmetric  $gg \rightarrow q\bar{q}$  background events which mostly distributes in the central region than that of the  $A_{\text{C}}$  [35]. Therefore  $A_{\text{E}}$  is usually more significant than the  $A_{\text{C}}$ . The difference between  $A_{\text{RFB}}$  and  $A_{\text{OFB}}$  is the cuts in order to keep the partonic asymmetry.  $Y_{f\bar{f}}$

and  $P_{f\bar{f}}^z$  are proportional to  $(x_1 - x_2)/(x_1 + x_2)$  and  $(x_1 - x_2)$  respectively, where  $x_1$  and  $x_2$  are the momentum fraction of the two colliding partons. The most important difference between the two categories is that the asymmetry utilizes the different kinematical information. The asymmetries in the first category utilize either  $f$  or  $\bar{f}$  momentum information. While the asymmetries of the second category require to measure the kinematical information of  $f$  and  $\bar{f}$  simultaneously.

Due to their different characteristics, the four types of asymmetries will be used in different cases. Each of them have their most suitable places. In the followings, we will investigate how to use four asymmetries to discriminate different  $Z'$  models, namely which one is the most suitable type of asymmetry and the corresponding optimal cuts.

### III. DISCRIMINATING DIFFERENT $Z'$ S VIA ASYMMETRIES

#### A. $Z'$ in the left-right model and sequential standard model

In this paper in order to illustrate how to utilize asymmetries to discriminate different  $Z'$ s, we choose two test models as the examples: left-right model and sequential standard model.

The left-right model is based on the symmetry group  $SU(2)_R \times SU(2)_L \times U(1)_{B-L}$ , where  $B - L$  is the difference between baryon and lepton numbers. The couplings between the  $Z'$  and fermions are [4, 6]

$$g_{Z'} J_{Z'}^\mu Z'_\mu = \frac{e}{c_W} \sum_f \bar{\psi}_f \gamma^\mu \left[ \frac{1 - \gamma^5}{2} g_L^{fZ'} + \frac{1 + \gamma^5}{2} g_R^{fZ'} \right] \psi_f Z'_\mu. \quad (7)$$

As the test model, the sequential standard model  $Z'$  has the same fermion couplings as the SM  $Z$  boson and which can be written as,

$$g_{Z'} J_{Z'}^\mu Z'_\mu = -\frac{g}{2c_W} \sum_f \bar{\psi}_f \gamma_\mu \left( g_V^f - g_A^f \gamma_5 \right) \psi_f Z'_\mu. \quad (8)$$

The parameters in these two models can be summarized in Tab. I. Throughout the paper the mass of  $Z'$  is set to be 1.5 TeV for both models. The  $\alpha_{LR}$  in LR model is set to be 1.88 as the benchmark point, in order to make the width of  $Z'$  in the LR model the same as that in the SSM. SM parameters are chosen as  $\alpha = 1/127.9$ ,  $\sin^2 \theta_W = 0.231$ ,  $M_Z = 91.133 \text{ GeV}$ ,  $\Gamma_Z = 2.495 \text{ GeV}$  and  $m_t = 171.2 \text{ GeV}$ . In calculating the width of the  $Z'$ , only its decays to the SM fermions are included.

TABLE I. Couplings of the  $Z'$  boson to the SM fermions in the left-right model and the sequential SM.  $\alpha_{LR} = \sqrt{(c_W^2 g_R^2 / s_W^2 g_L^2) - 1}$ , where  $g_L = e/s_W$  and  $g_R$  are the  $SU(2)_L$  and  $SU(2)_R$  coupling constants with  $s_W^2 = 1 - c_W^2 \equiv \sin^2 \theta_W$  [4].

$f$	$g_L^{fZ'}$	$g_R^{fZ'}$	$g_V^f$	$g_A^f$
$e$	$\frac{1}{2\alpha_{LR}}$	$\frac{1}{2\alpha_{LR}} - \frac{\alpha_{LR}}{2}$	$-\frac{1}{2} + 2\sin^2 \theta_W$	$-\frac{1}{2}$
$u$	$-\frac{1}{6\alpha_{LR}}$	$-\frac{1}{6\alpha_{LR}} + \frac{\alpha_{LR}}{2}$	$\frac{1}{2} - \frac{4}{3}\sin^2 \theta_W$	$\frac{1}{2}$
$d$	$-\frac{1}{6\alpha_{LR}}$	$-\frac{1}{6\alpha_{LR}} - \frac{\alpha_{LR}}{2}$	$-\frac{1}{2} + \frac{2}{3}\sin^2 \theta_W$	$-\frac{1}{2}$

## B. Optimizing asymmetry

In our analysis, the basic kinematical cuts are taken as  $p_T > 20\text{GeV}$  and  $Y < 2.5$  for the leptons,  $p_T > 0.3M_{Z'}$  and  $Y < 2.5$  for the bottom and top quarks. Here the  $p_T$  cut for quarks can suppress the QCD backgrounds. The LHC energy  $\sqrt{s}$  is set to be 14 TeV.

Fig. 1 shows  $A_{\text{RFB}}$  for the process  $pp \rightarrow e^+e^-X$  as a function of  $M_{e^+e^-}$ . From the figure it is clear that the asymmetry depends on  $M_{e^+e^-}$ . As depicted above, the asymmetry depends on the chiral properties of  $Z'$  and SM fermions, as well as the selected data sample. In order to keep the asymmetry information as much as possible, in our analysis the four data samples are chosen, same with those in Ref. [8]. They are the on-peak events with  $M_{Z'} - 3\Gamma < M_{\mu^+\mu^-(e^+e^-)} < M_{Z'} + 3\Gamma$ , off-peak events with  $2/3M_{Z'} < M_{\mu^+\mu^-(e^+e^-)} < M_{Z'} - 3\Gamma$ , on-peak events with  $M_{Z'} - 2.5\Gamma < M_{b\bar{b}} < M_{Z'} + 2.5\Gamma$  and on-peak events with  $M_{Z'} - 2.5\Gamma < M_{t\bar{t}} < M_{Z'} + 2.5\Gamma$ .

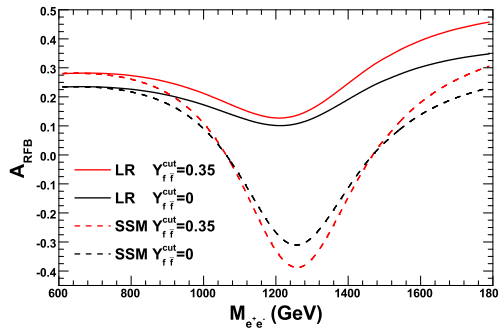


FIG. 1.  $A_{\text{RFB}}$  for the process  $pp \rightarrow e^+e^-X$  as a function of  $M_{e^+e^-}$  in LR mode and SSM with cuts  $Y_{f\bar{f}}^{\text{cut}} = 0$  and  $Y_{f\bar{f}}^{\text{cut}} = 0.35$  respectively.



From Fig. 1  $A_{\text{RFB}}$  with  $Y_{ff}^{\text{cut}} = 0.35$  is larger than that with  $Y_{ff}^{\text{cut}} = 0$ . However the magnitude of  $A_{\text{RFB}}$  is not a good measure to optimize the observable. As usual we utilize the significance of the asymmetry as a measure to select optimal cuts. The significance is defined as

$$S_A \equiv \frac{\sigma^A \mathcal{L}}{\sqrt{\sigma \mathcal{L}}} = A_{\text{FB}} \sqrt{\mathcal{L} \sigma}, \quad (9)$$

where  $A_{\text{FB}}$  can be  $A_{\text{RFB}}$ ,  $A_{\text{OFB}}$ ,  $A_C$  or  $A_E$ ,  $\mathcal{L}$  is the LHC integrated luminosity which is taken as  $100\text{fb}^{-1}$  throughout our analysis, and  $\sigma$  is the cross section. In this part, the detection efficiency is set to be 1.

Figs. 2, 3, 4 and 5 show the significance as a function of the corresponding cut for four asymmetries and four data samples respectively. In order to achieve the maximum significance the corresponding best cuts are depicted in Tabs. II, III, IV and V respectively.

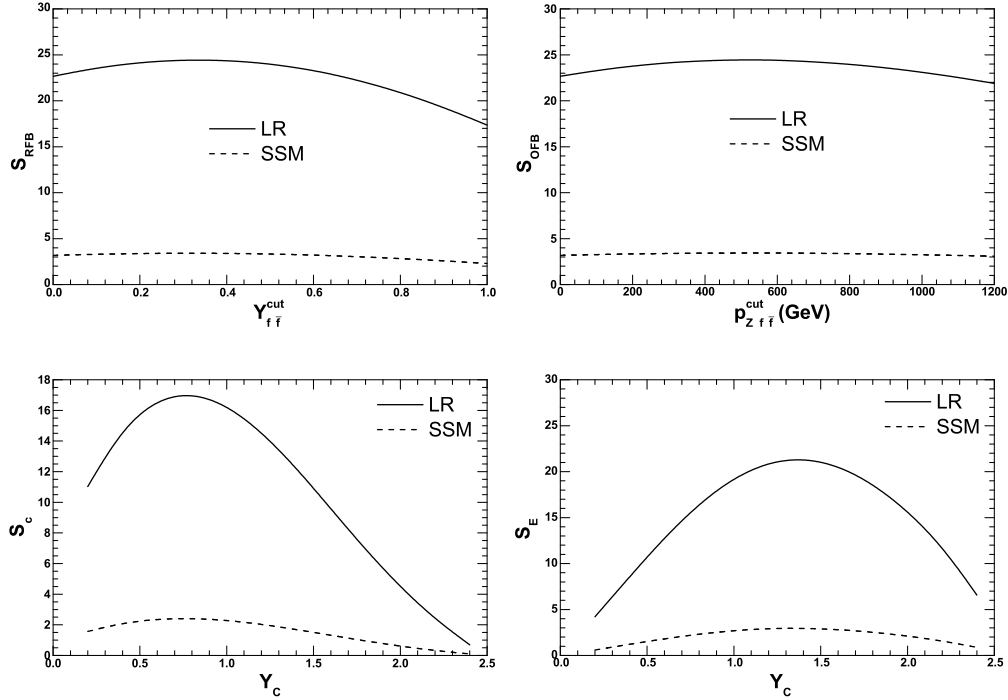
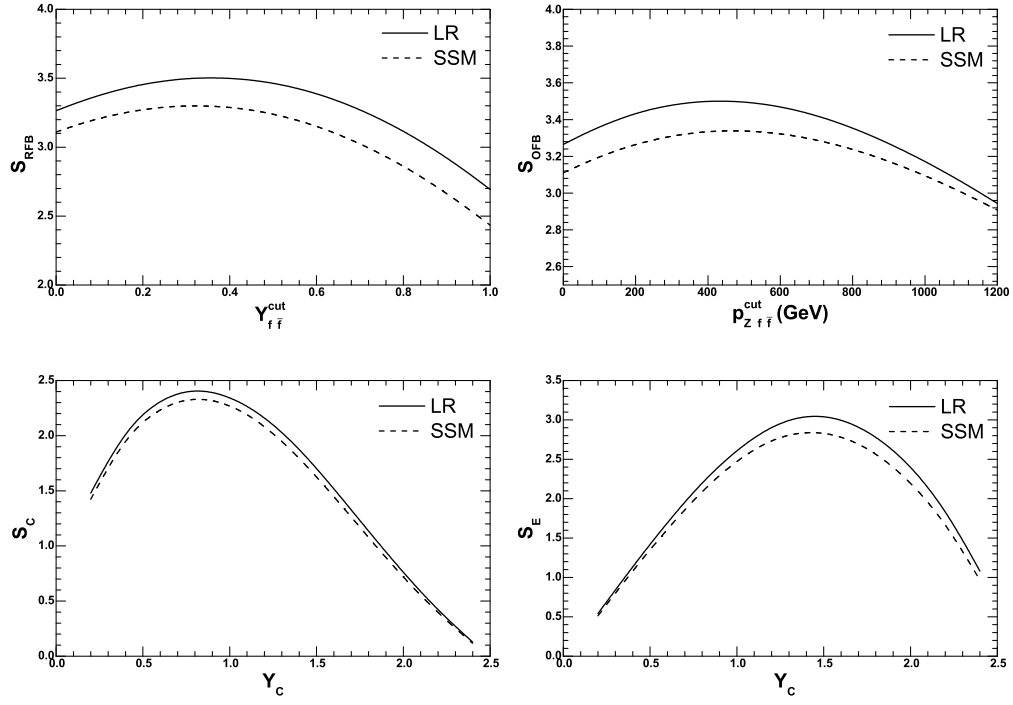
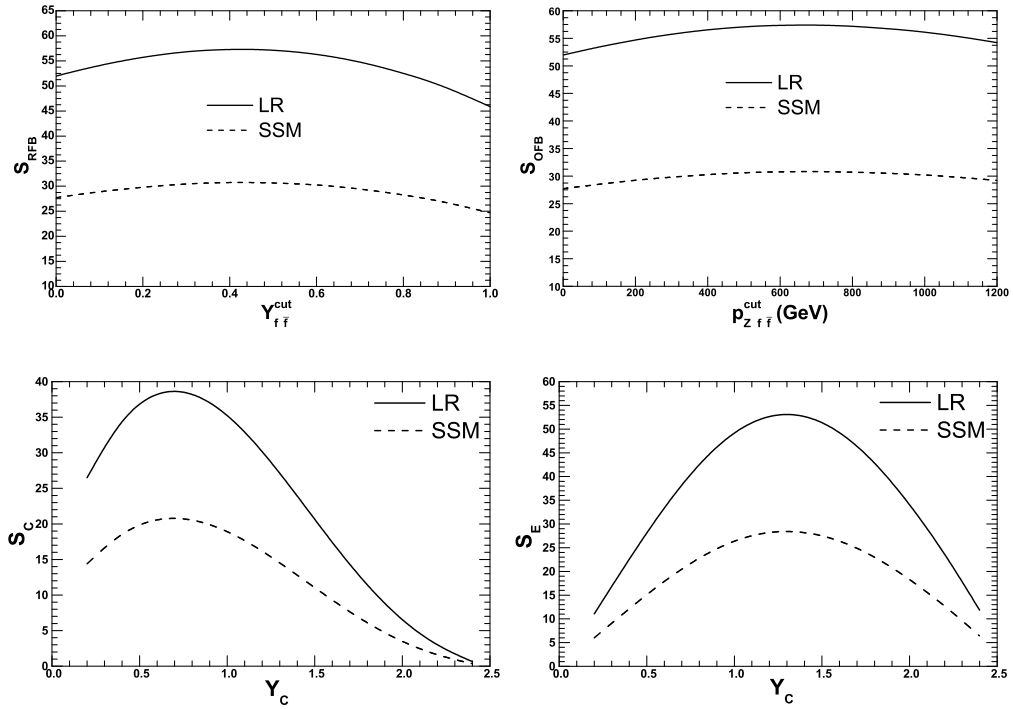
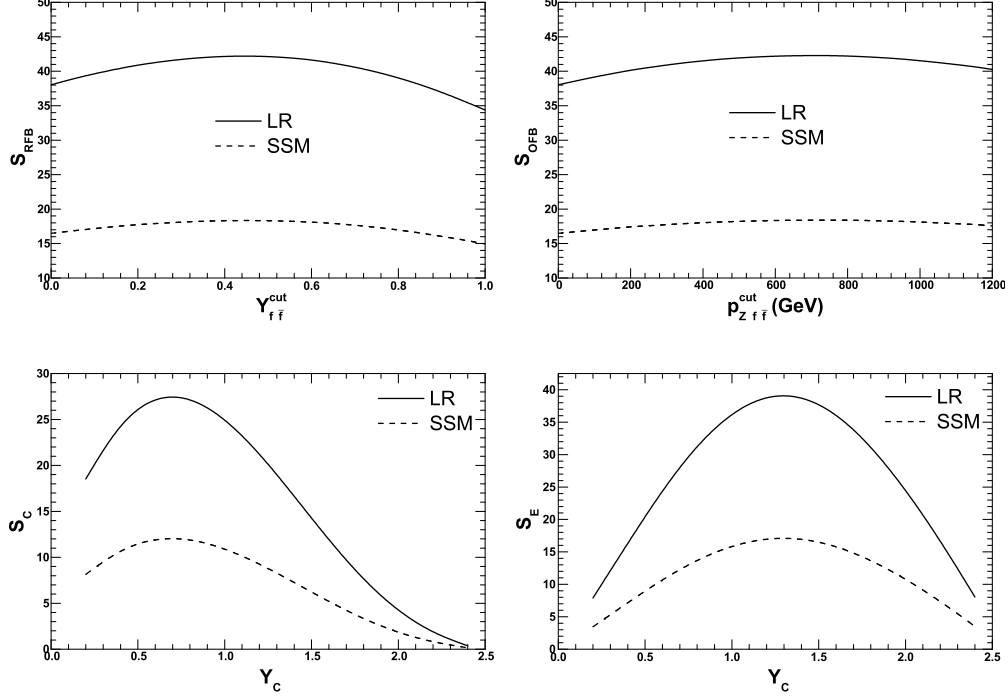


FIG. 2. Significance as a function of corresponding cut for on-peak  $e^+e^-$  events in LR model and SSM.

Generally speaking, the significance of the LR model is always greater than that of the SSM in the benchmark parameters we choose.  $S_{\text{RFB}}$  and  $S_{\text{OFB}}$  are not so sensitive to the cuts as those of  $S_C$  and  $S_E$ . Their maximum values are almost the same. At the same

FIG. 3. Same with Fig. 2 except for off-peak  $e^+e^-$  events.FIG. 4. Same with Fig. 2 except for on-peak  $b\bar{b}$  events.

FIG. 5. Same with Fig. 2 except for on-peak  $t\bar{t}$  events.TABLE II. Optimized cut and the corresponding maximum value of significance for on-peak  $e^+e^-$  events for the four kinds of asymmetries in both LR model and SSM.

LR				
	$A_{\text{RFB}}$	$A_{\text{OFB}}$	$A_{\text{C}}$	$A_{\text{E}}$
Best cut	$Y_{\text{cut}}^{f\bar{f}} = 0.35$	$P_{z,\text{cut}}^{f\bar{f}} = 550\text{GeV}$	$Y_{\text{C}} = 0.8$	$Y_{\text{C}} = 1.4$
Significance(with $100\text{fb}^{-1}$ )	24.4	24.4	17.1	21.5
SSM				
	$A_{\text{RFB}}$	$A_{\text{OFB}}$	$A_{\text{C}}$	$A_{\text{E}}$
Best cut	$Y_{\text{cut}}^{f\bar{f}} = 0.35$	$P_{z,\text{cut}}^{f\bar{f}} = 550\text{GeV}$	$Y_{\text{C}} = 0.8$	$Y_{\text{C}} = 1.4$
Significance(with $100\text{fb}^{-1}$ )	3.40	3.43	2.43	2.97

time the optimized cuts are the same for the two test models although their magnitudes are different. The reason is that the optimal cuts depend mainly on the properties of the parton distribution function and mass of the  $Z'$ . Therefore the optimal cuts are nearly independent on the chiral properties of  $Z'$  coupling to fermions. The optimized cuts obtained from one specific  $Z'$  model are applicable to any other  $Z'$  model with the same  $Z'$  mass.

TABLE III. Same with Tab. II except for off-peak  $e^+e^-$  events.

LR				
	$A_{RFB}$	$A_{OFB}$	$A_C$	$A_E$
Best cut	$Y_{\text{cut}}^{f\bar{f}} = 0.35$	$P_{z,\text{cut}}^{\bar{f}f} = 450\text{GeV}$	$Y_C = 0.8$	$Y_C = 1.4$
Significance(with $100\text{fb}^{-1}$ )	3.51	3.51	2.43	3.07
SSM				
	$A_{RFB}$	$A_{OFB}$	$A_C$	$A_E$
Best cut	$Y_{\text{cut}}^{f\bar{f}} = 0.35$	$P_{z,\text{cut}}^{\bar{f}f} = 450\text{GeV}$	$Y_C = 0.8$	$Y_C = 1.4$
Significance(with $100\text{fb}^{-1}$ )	3.30	3.34	2.36	2.87

TABLE IV. Same with Tab. II except for on-peak  $b\bar{b}$  events.

LR				
	$A_{RFB}$	$A_{OFB}$	$A_C$	$A_E$
Best cut	$Y_{\text{cut}}^{f\bar{f}} = 0.45$	$P_{z,\text{cut}}^{\bar{f}f} = 700\text{GeV}$	$Y_C = 0.6$	$Y_C = 1.2$
Significance(with $100\text{fb}^{-1}$ )	57.2	57.4	38.8	53.1
SSM				
	$A_{RFB}$	$A_{OFB}$	$A_C$	$A_E$
Best cut	$Y_{\text{cut}}^{f\bar{f}} = 0.45$	$P_{z,\text{cut}}^{\bar{f}f} = 700\text{GeV}$	$Y_C = 0.6$	$Y_C = 1.2$
Significance(with $100\text{fb}^{-1}$ )	30.7	30.8	20.9	28.5

In LR model or SSM,  $A_{OFB}$  and  $A_{RFB}$  can obtain almost the same highest significance values. Significance of  $A_E$  is smaller and significance of  $A_C$  is the smallest. The reason is that  $A_E$  and  $A_C$  defined in the laboratory frame are diluted by the longitudinal boosts from the partonic level to the hadron level.  $A_C$  is even smaller because it includes more symmetric backgrounds than that of  $A_E$ . Note that these results are based on the assumption that the final  $f\bar{f}$  pair can be completely reconstructed. In the real experiment, taking the top quark pair as the example, the momentum precision of the top pair will be limited by the missing neutrino when using the top semi-leptonically decaying mode [36]. While  $A_E$  and  $A_C$  can be free from this problem because they utilize only the top or anti-top hadronic decay mode.

TABLE V. Same with Tab. II except for on-peak  $t\bar{t}$  events.

LR				
	$A_{\text{RFB}}$	$A_{\text{OFB}}$	$A_{\text{C}}$	$A_{\text{E}}$
Best cut	$Y_{\text{cut}}^{f\bar{f}} = 0.45$	$P_{z,\text{cut}}^{\text{f}\bar{\text{f}}} = 700\text{GeV}$	$Y_{\text{C}} = 0.6$	$Y_{\text{C}} = 1.2$
Significance(with $100\text{fb}^{-1}$ )	42.2	42.3	27.6	39.2
SSM				
	$A_{\text{RFB}}$	$A_{\text{OFB}}$	$A_{\text{C}}$	$A_{\text{E}}$
Best cut	$Y_{\text{cut}}^{f\bar{f}} = 0.45$	$P_{z,\text{cut}}^{\text{f}\bar{\text{f}}} = 700\text{GeV}$	$Y_{\text{C}} = 0.6$	$Y_{\text{C}} = 1.2$
Significance(with $100\text{fb}^{-1}$ )	18.3	18.4	12.1	17.1

### C. Discriminating $Z'$ models utilizing the optimized asymmetry

Based on the optimal cuts obtained above, we can discriminate different  $Z'$ s via the precise asymmetry measurements at the LHC. In this part we calculated the asymmetries and compare the optimal and un-optimal cases. The results for all asymmetries can be deduced in the same procedure. Note that the optimized cuts are almost the same for different  $Z'$  models provided that the  $Z'$  mass is the same.

To identify the candidate  $Z'$  model, the measured asymmetry should be compared with the theoretical predictions. In our analysis, asymmetries by theoretical predictions with errors are presented as the two-dimensional plot, similar to that in Ref. [8].

In Fig. 6 we show the different asymmetries for both LR model and the SSM. Central values are calculated in both optimized and un-optimized cases. The error bar are estimated according to the formula

$$\text{err} \equiv \sqrt{\frac{4N^F N^B}{N^3}} = \frac{1}{\sqrt{N}} \sqrt{1 - \left(\frac{N^A}{N}\right)^2} \cong \frac{1}{\sqrt{\mathcal{L}\sigma\epsilon_{f\bar{f}}}}. \quad (10)$$

Here  $N^F/N^B$  is the forward/backward events,  $N^A = N^F - N^B$  is the asymmetric events and  $N$  is the total events. The relation between err and significance is  $S_A = A_{\text{FB}}/\text{err}$ , where  $S_A$  is the significance with reconstruction efficiency. In our estimation, the  $b\bar{b}$  and  $t\bar{t}$  reconstruction efficiencies are taken as  $\epsilon_{b\bar{b}} = 0.36$  and  $\epsilon_{t\bar{t}} = 0.075$  respectively [8]. For the  $b\bar{b}$  and  $t\bar{t}$  final states, next-to-leading order QCD contribution to the asymmetric cross sections are included. For the  $b\bar{b}$  final state, QCD NLO contribution to on-peak  $A_{\text{RFB}}$  is 1.38% for the optimized case and 0.96% for the un-optimized  $Y_{\text{cut}}^{\text{f}\bar{\text{f}}} = 0$  case. The contribution is a

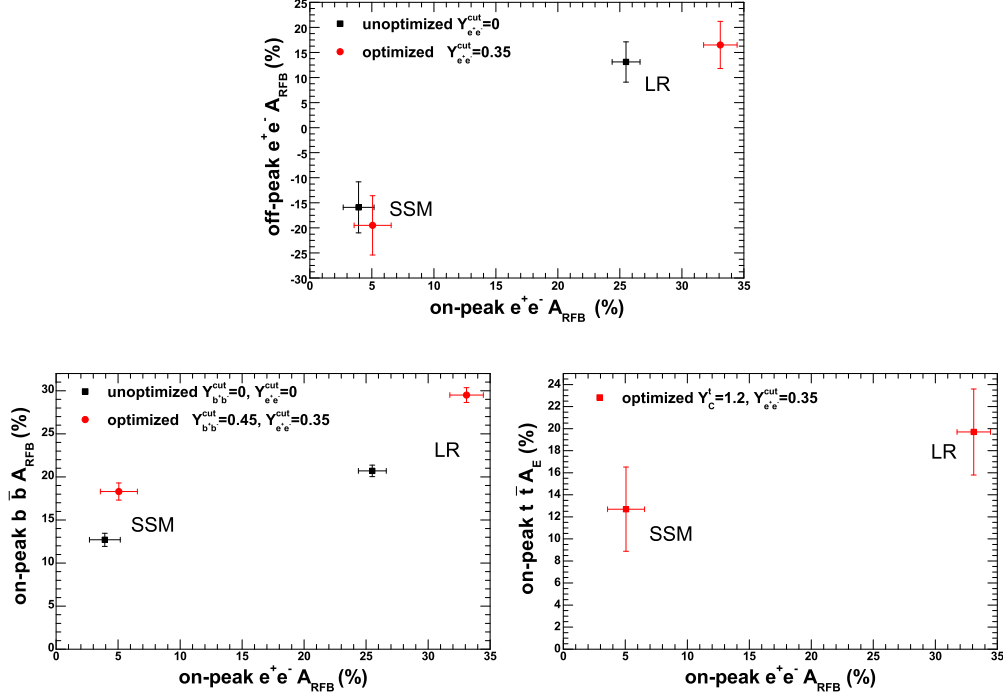


FIG. 6. Two dimensional plots of asymmetries  $A_{RFB}$ s for off- and on-peak  $e^+e^-$  events,  $A_{RFB}$ s for on-peak  $b\bar{b}$  and  $e^+e^-$  events, and  $A_E$  and  $A_{RFB}$  for on-peak  $t\bar{t}$  and  $e^+e^-$  events respectively. Both optimized and un-optimized results for  $A_{RFB}$  and optimized ones for  $A_E$  with error bars in the LR model and SSM are presented.

little bit larger than the statistic error (see the left-bottom diagram of Fig. 6), so this effect should be taken into account. For the  $t\bar{t}$  final states, QCD NLO contribution to on-peak  $A_E$  is 0.53% for the optimized case, which is much less than the statistic error (see the right-bottom diagram of Fig. 6), so this effect can be neglected.

From the Fig. 6, the two models give the apparently different predictions for two asymmetries. Even without optimal cuts, the asymmetries can be utilized to discriminate models in this case. However in the real case, the asymmetry difference for various models might be small. In this case the optimal cuts can help to improve the capacity to discriminate models. From the figure it is obviously that the central values of the asymmetries separate more apart in both the LR model and the SSM. However, due to the decreasing of the statistics, the error bar becomes a little bit larger for the optimized case.

#### IV. DISCUSSIONS AND CONCLUSIONS

In this paper we investigated how to utilize the asymmetry measurements at the LHC to discriminate underlying dynamics, by taking  $Z'$  model as the example. Unlike LEP and Tevatron, the LHC is a symmetric proton-proton collider, thus the asymmetry at the LHC has the unique feature which should be studied in detail. In literature several asymmetries have been proposed at the LHC, namely rapidity-dependent forward-backward asymmetry, one-side forward-backward asymmetry, central charge asymmetry and edge charge asymmetry, with  $\ell^+\ell^-$ ,  $b\bar{b}$  and  $t\bar{t}$  as the final states. Based on these works, we stepped further on to analyze how to optimize the asymmetries in the left-right model and the sequential standard model. In the calculations with  $b\bar{b}$  and  $t\bar{t}$  final states, the QCD-induced higher order contributions to the asymmetric cross section were also included. For each kind of final states, we estimated the four kinds of asymmetries and especially the optimal cuts usually associated with the definition of the asymmetry. Our studies showed that the optimal cut is stable for different  $Z'$  model provided that the  $Z'$  mass is equal. The numerical results indicated that the capacity to discriminate  $Z'$  models can be improved by imposing the optimal cuts.

In this paper only  $Z'$  models of left-right and sequential standard model were investigated as the examples. However the optimization obtained from these two examples is suitable for any kind of  $Z'$  models provided that they have the same  $Z'$  mass. The  $Z'$  mass throughout this paper is assumed to be 1.5 TeV as the benchmark parameter. If the  $Z'$  mass is other than 1.5 TeV, the optimal condition should be investigated in the same procedure. Moreover precise asymmetry measurement at the LHC can be utilized to scrutinize any new dynamics beyond the standard model, not limited to the  $Z'$  case.

#### ACKNOWLEDGMENT

This work was supported in part by the Natural Science Foundation of China (No 11075003).

- 
- [1] P. Langacker, R. W. Robinett, and J. L. Rosner, Phys. Rev. D **30**, 1470 (1984).
  - [2] M. Cvetič and S. Godfrey, (1995), arXiv: hep-ph/9504216.

- [3] M. Dittmar, Phys. Rev. D **55**, 161 (1997).
- [4] M. Dittmar, A.-S. Nicollerat, and A. Djouadi, Phys. Lett. **B583**, 111 (2004), arXiv: hep-ph/0307020.
- [5] S. Godfrey and T. A. W. Martin, Phys. Rev. Lett. **101**, 151803 (2008).
- [6] F. Petriello and S. Quackenbush, Phys. Rev. D **77**, 115004 (2008).
- [7] P. Langacker, Rev. Mod. Phys. **81**, 1199 (2009).
- [8] R. Diener, S. Godfrey, and T. A. W. Martin, (2009), arXiv: 0910.1334.
- [9] R. Diener, S. Godfrey, and T. A. W. Martin, Phys. Rev. D **80**, 075014 (2009).
- [10] R. Diener, S. Godfrey, and T. A. W. Martin, (2010), arXiv: 1006.2845.
- [11] V. Barger and K. Whisnant, Phys. Rev. D **36**, 979 (1987).
- [12] F. del Aguila, M. Quiros, and F. Zwirner, Nucl. Phys. **B287**, 419 (1987).
- [13] V. Barger, N. G. Deshpande, J. L. Rosner, and K. Whisnant, Phys. Rev. D **35**, 2893 (1987).
- [14] U. Baur and K. H. Schwarzer, Phys. Lett. **B180**, 163 (1986).
- [15] S. Godfrey, J. L. Hewett, and T. G. Rizzo, Phys. Rev. D **37**, 643 (1988).
- [16] J. L. Rosner, Phys. Lett. **B221**, 85 (1989).
- [17] F. Boudjema, F. M. Renard, and C. Verzegnassi, Phys. Lett. **B202**, 411 (1988).
- [18] J. D. Anderson, M. H. Austern, and R. N. Cahn, Phys. Rev. D **46**, 290 (1992).
- [19] M. Cvetič and P. Langacker, Phys. Rev. **D46**, 14 (1992).
- [20] P. Langacker and M. Luo, Phys. Rev. D **45**, 278 (1992).
- [21] F. Feruglio, Presented at 26th Rencontres de Moriond, Les Arcs, France, Mar 10-17, 1991.
- [22] C. Verzegnassi, Invited Seminar at Beyond the Standard Model, Int. Europhysics Conf. on High Energy Physics, Uppsala, Sweden, Jun 25 - Jul 1, 1987.
- [23] J. L. Rosner, In Proc. of 1986 Summer Study on the Physics of Superconducting Super Collider, Snowmass, CO, Jun 23 - Jul 11, 1986.
- [24] J. L. Rosner, Phys. Rev. D **54**, 1078 (1996).
- [25] F. del Aguila, M. Cvetič, and P. Langacker, Phys. Rev. D **48**, R969 (1993).
- [26] DELPHI, J. Abdallah *et al.*, Eur. Phys. J. **C45**, 589 (2006), arXiv: hep-ex/0512012.
- [27] P. Langacker, (2009), arXiv: 0911.4294.
- [28] S. Gopalakrishna, T. Han, I. Lewis, Z.-g. Si, and Y.-F. Zhou, Phys. Rev. D **82**, 115020 (2010).
- [29] J. H. Kühn and G. Rodrigo, Phys. Rev. Lett. **81**, 49 (1998).
- [30] J. H. Kühn and G. Rodrigo, Phys. Rev. D **59**, 054017 (1999).



- [31] O. Antuñano, J. H. Kühn, and G. Rodrigo, Phys. Rev. D **77**, 014003 (2008).
- [32] P. Ferrario and G. Rodrigo, Phys. Rev. D **78**, 094018 (2008).
- [33] Y.-k. Wang, B. Xiao, and S.-h. Zhu, Phys. Rev. D **82**, 094011 (2010).
- [34] Y.-k. Wang, B. Xiao, and S.-h. Zhu, (2010), Phys. Rev. D **83**, 015002 (2011).
- [35] B. Xiao, Y.-K. Wang, Z.-Q. Zhou, and S.-h. Zhu, (2011), arXiv: 1101.2507.
- [36] The CDF, T. Aaltonen *et al.*, (2011), 1101.0034.